ISSN 1063-7850, Technical Physics Letters, 2012, Vol. 38, No. 5, pp. 439–442. © Pleiades Publishing, Ltd., 2012.
Original Russian Text © M.R. Ainbund, A.N. Alekseev, O.V. Alymov, V.N. Jmerik, L.V. Lapushkina, A.M. Mizerov, S.V. Ivanov, A.V. Pashuk, S.I. Petrov, 2012, published in Pis'ma v Zhurnal Tekhnicheskoi Fiziki, 2012, Vol. 38, No. 9, pp. 88–95.

Solar-Blind UV Photocathodes Based on AlGaN Heterostructures with a 300- to 330-nm Spectral Sensitivity Threshold

M. R. Ainbund, A. N. Alekseev, O. V. Alymov, V. N. Jmerik, L. V. Lapushkina, A. M. Mizerov, S. V. Ivanov, A. V. Pashuk, and S. I. Petrov*

ELECTRON Central Research Institute, St. Petersburg, 194223 Russia
Semiconductor Technologies and Equipment Company (SemiTEq), St. Petersburg, 194156 Russia
Ioffe Physical Technical Institute, Russian Academy of Sciences, St. Petersburg, 194021 Russia
**e-mail: petrov@semiteq.ru*

Received October 24, 2011

Abstract—Solar-blind UV photodetectors based on photocathodes are among the important applications of heterostructures based on group III metal nitride semiconductors. Related investigations are most frequently devoted to photocathodes with *p*-GaN active regions characterized by a long-wavelength sensitivity threshold at 360 nm. Since the detected radiation is mostly concentrated in the spectral range below 240–290 nm, corresponding displacement of the long-wavelength sensitivity threshold of photodetectors by using photocathodes with *p*-AlGaN active regions is a topical task. We present preliminary results on manufacturing photocathodes with a *p*-$Al_xGa_{1-x}N$ ($x = 0.1$ and 0.3) active region (possessing a long-wavelength sensitivity threshold at 330 and 300 nm, respectively).

DOI: 10.1134/S1063785012050033

Optical systems operating in the UV spectral range are widely used for observation of astronomical and cosmic objects, high-voltage electric discharges, flames, laser and plasma plumes, etc. Maximum sensitivity of photodetectors for these systems should be provided in a wavelength interval of 240–290 nm, since the emission with shorter wavelengths is strongly absorbed in the atmosphere, while longer wavelengths occupy a significant part of the solar radiation spectrum [1]. Of the photodetectors meeting these requirements (revered to as solar blind), photocathodes based on alkali metal tellurides Cs_2Te and Rb_2Te have been most widely employed. In recent years, in addition to devices based on these compounds, some alternative semiconductor photocathodes with negative electron affinity have been actively developed using epitaxial heterostructures based on wide-bandgap group III metal nitrides, in particular AlGaN. It is expected that the quantum yield (Y) and the slope of the photosensitivity decay near the visible spectral range in photocathodes based on this compound can be significantly increased. An important additional advantage of devices based on $Al_xGa_{1-x}N$ compounds is the possibility of controlling the long-wavelength sensitivity threshold within 360–200 nm by changing the solid solution composition (i.e., by varying x within 0–1). However, to the best of the authors' knowledge, most investigations have been devoted to the development of photocathodes based on structures employing GaN:Mg binary compound, which is characterized by a long-wavelength sensitivity threshold fixed at 360 nm [2, 3]. Despite the conventionally mentioned importance of shifting this threshold toward shorter wavelengths, very few experimental data have been reported on development of these photocathodes [4].

This Letter presents data on the fabrication of solar-blind photocathodes with active regions based on $Al_{0.1}Ga_{0.9}N$:Mg and $Al_{0.3}Ga_{0.7}N$:Mg, which are characterized by a short-wavelength shift of the spectral sensitivity threshold as compared to that in analogous structures based on the binary GaN compound.

AlGaN heterostructures were grown by molecular beam epitaxy (MBE) using active nitrogen supplied either via high-temperature cracking of ammonia or via plasma activation of molecular nitrogen. MBE growth was carried out in two stages—respectively, in an STE-3N2 setup (Semiconductor Technologies and Equipment (SemiTEq), St. Petersburg) at the SemiTEq Applied Research Laboratory and in a Compact 21T system (Riber, France) at the Physical Technical Institute. In the former case, sequentially deposited AlGaN/AlN buffer layers with a total thickness of ~1 μm were formed on c-Al_2O_3 substrates at extremely high substrate temperatures (T_s = 950–1150°C), which allowed the density of dislocations in the active region to be reduced to 8×10^8–1×10^9 cm^{-2} [5]. Then, the substrate with a buffer layer was transferred to the second setup. After short-term annealing in vacuum at 700°C, active layers of $Al_xGa_{1-x}N$:Mg with different contents of aluminum ($x = 0.1$ and 0.3) were grown under metal-rich stoichiometry conditions at

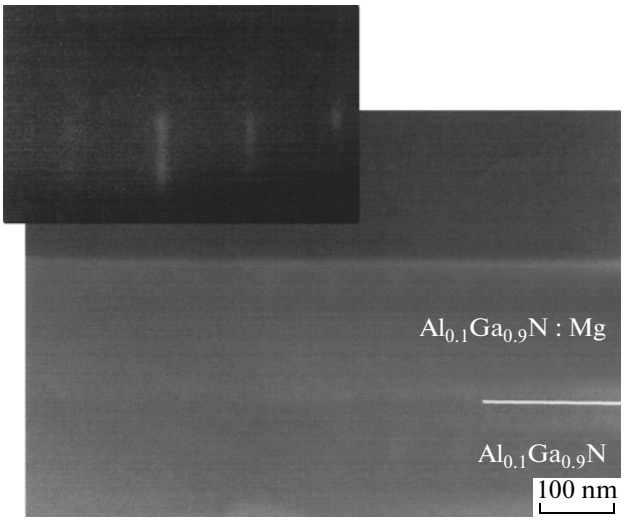

Fig. 1. SEM image of the near-surface region of a heterostructure with an active (uppermost) $Al_{0.1}Ga_{0.9}N$:Mg layer. The inset shows the characteristic linear RHEED pattern, which was observed during the entire growth of this layer.

a relatively low substrate temperature (T_s = 650°C) and the same flux of Mg atoms from a solid-state effusion source as described in detail elsewhere [6]. The active layer thickness was within 200–250 nm. Finally, the heterostructures were subjected to postgrowth treatment in a special setup at the ELECTRON Central Research Institute. The samples were cleaned in a vacuum chamber of this setup with a residual pressure of 5×10^{-11} Torr by heating in vacuum and activated with cesium and oxygen according to the technique described in [7].

Heterostructures with doped AlGaN:Mg layers were characterized at the intermediate stage by the methods of scanning electron microscopy (SEM), reflection high-energy electron diffraction (RHEED), secondary ion mass spectroscopy (SIMS), low-temperature (20 K) photoluminescence (PL) spectroscopy, and PL excitation spectroscopy (using a Xe lamp with a minimum wavelength of $\lambda = 260$ nm).

Figure 1 shows an SEM image of the near-surface region of a heterostructure with an active (uppermost) $Al_{0.1}Ga_{0.9}N$:Mg layer, which was measured prior to postgrowth activation treatment. As can be seen, there is a sharp contrast between the doped and undoped layers. In addition, the SEM image shows evidence of a planar morphology of the active layer surface. The atomically smooth character of this surface was also confirmed by the linear RHEED pattern, which was observed during the entire growth cycle (see the inset to Fig. 1). Analogous SEM contrast and surface morphology were observed for a structure with the $Al_{0.3}Ga_{0.7}N$:Mg active region. The results of SIMS measurements showed that the concentration of Mg in the near-surface layers was $\sim 1 \times 10^{19}$ cm^{-3}.

Figure 2 (curve *1*) presents the PL excitation spectrum measured for the $Al_{0.3}Ga_{0.7}N$:Mg active layer with the emission detected at $\lambda = 360$ nm, i.e., in the region of a low-energy band in the PL spectrum (curve *2*). Using this spectrum, it is possible to estimate the bandgap width of the active layer as ~4.1 eV, which approximately corresponds to the composition of a ternary AlGaN:Mg compound that was preset during growth [8]. The main peak in the PL spectrum of this layer ($\lambda = 360$ nm) can be assigned to recombination of donor–acceptor pairs. It is also necessary to note a strong shift of the position of this peak relative to the absorption edge (the difference amounting to ~700 meV), in contrast to the case of GaN:Mg layers, where the analogous energy difference (for the same Mg concentration) is ~200 meV [9]. The position of this peak in the AlGaN:Mg ternary compound is determined by several factors, including (i) growth in the energy of ionization of the acceptor impurity with increasing Al content [10], (ii) localization of charge carriers on fluctuations of the solid solution composition, and (iii) nonuniform distribution of Mg atoms [11]. Further investigations of the optical properties of AlGaN:Mg layers are in progress.

Figure 3a shows the spectra of the quantum efficiency of $Al_{0.1}Ga_{0.9}N$:Mg and $Al_{0.3}Ga_{0.7}N$:Mg structures illuminated from the front (curves *1* and *3*) and rear (curves *4* and *5*) sides, respectively, as measured in the working chamber. Under illumination from the front side, the quantum efficiency reaches a rather high level of Y = 10–25%, while the photoemission thresholds are shifted to $\lambda = 330$ and 300 nm, respectively. For illumination from the rear side, the sensitivity is much lower and exhibits sharp maxima at $\lambda = 340$ and 300 nm (curves *4* and *5*, respectively). This behavior of spectral characteristics is related to the absorption of radiation transmitted through the buffer layer, since the content of aluminum in the upper part of the buffer layer is the same as that in the active *p*-AlGaN region. These data are presented here, since they point to the possibility of obtaining narrow-bandgap photodetectors by making the aluminum content in the upper part of the buffer layer slightly greater than in the active region.

One $Al_{0.1}Ga_{0.9}N$:Mg structure with lateral dimensions 12 × 12 mm was used to manufacture a prototype photodetector with a magnesium fluoride entrance window. Figure 3a (curve *2*) shows the spectrum of the quantum efficiency of this device. This photodetector was also used to measure the nonuniformity of the spectral sensitivity over the photocathode area. This was achieved by irradiating from the device from the front side by radiation with $\lambda = 250$ nm via a diaphragm with a 1-mm-diameter hole that could be moved over the photocathode in two mutually perpendicular directions (vertical and horizontal). As can be seen from Fig. 3b, the nonuniformity of the spectral sensitivity over a length of 8 mm was within ±15%,

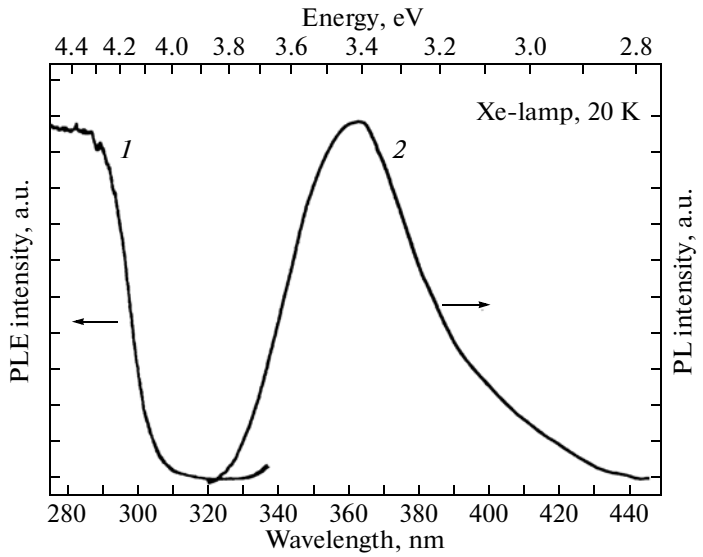

Fig. 2. Low-temperature (20 K) PL excitation spectrum of the $Al_{0.3}Ga_{0.7}N$:Mg layer (curve *1*) with the emission detected at $\lambda = 360$ nm, i.e., in the region of a low-energy band in the PL spectrum (curve *2*).

which is evidence of a high homogeneity of the properties of the heterostructure studied.

An important problem that hinders the creation of effective photocathodes with a long-wavelength sensitivity threshold below 360 nm is a decrease in the efficiency of doping in the active *p*-AlGaN region with increasing Al content, which is related to an increase in the ionization energy [10]. As can be seen from Fig. 3a, the quantum efficiency of samples with an aluminum content of 10 and 30% in the region of the long-wavelength sensitivity threshold is approximately on the same level, which is probably indicative of a sufficiently high doping level. At present, investigations are carried out to provide for optimization of the AlN/AlGaN buffer layer so as to reduce the density of dislocations in the active region (as compared to that in the standard AlN layer), on one hand, and to retain the necessary level of transmission in the working UV range for the obtaining of effective photocathodes, on the other hand.

Thus, we have presented data on the first domestic photocathodes operating in the reflection mode, which are based on *p*-$Al_xGa_{1-x}N$ ($x = 0.1$ and 0.3) heterostructures. It is established that an increase in the content of Al in the active region allows the long-wavelength sensitivity threshold to be decreased from 330 to 300 nm. At present, investigations aimed at optimization of the AlN/AlGaN buffer layer are being carried out so as to obtain an effective photocathode with a long-wavelength sensitivity threshold below 300 nm in the transmission mode.

Acknowledgments. Investigations at Semiconductor Technologies and Equipment Co. (St. Petersburg) were supported in part by the Ministry of Education

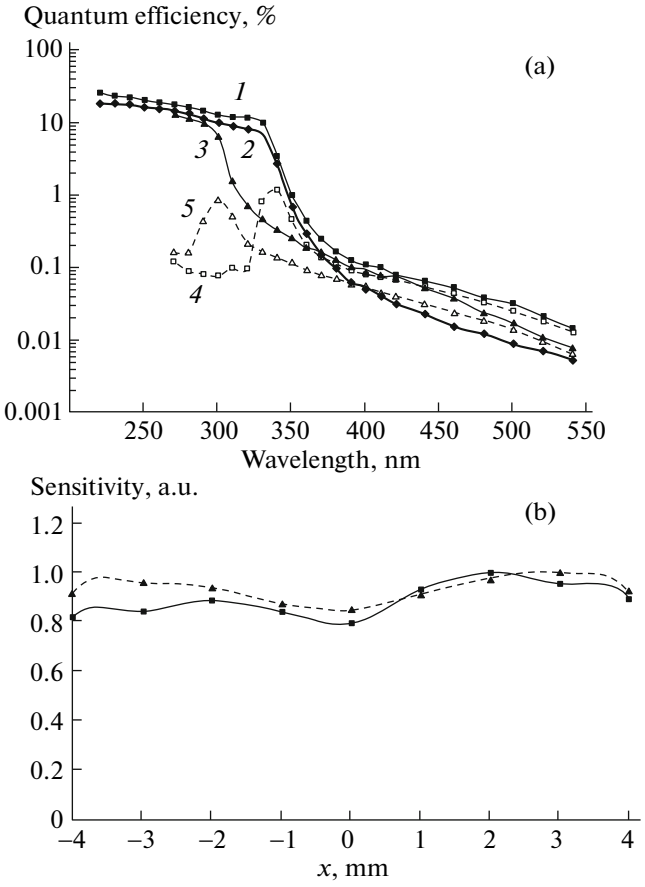

Fig. 3. (a) Plots of quantum efficiency vs. emission wavelength for (*1*, *2*, *4*) $Al_{0.1}Ga_{0.9}N$:Mg and (*3*, *5*) $Al_{0.3}Ga_{0.7}N$:Mg samples illuminated from the (*1*, *3*) front and (*4*, *5*) rear sides in the working chamber and (*2*) in a prototype photodetector; (b) dependence of the photocathode sensitivity at $\lambda = 250$ nm on the position of a diaphragm moved in two mutually perpendicular directions over the prototype photodetector.

and Science of the Russian Federation, project no. 02.523.11.3019.

REFERENCES

1. M. R. Ainbund, I. N. Surikov, O. V. Chernova, and V. V. Chikunov, Vopr. Radioelektron., Ser. Tekhn. Televid., No. 1, 69 (2007).
2. O. Siegmund, J. Vallerga, K. McPhate, J. Malloiy, A. Tremsin, A. Martin, M. Ulmer, and B. Wessels, Nucl. Instrum. Meth. Phys. Res. A **567**, 89 (2006).
3. X. Wang, B. Chang, R. Ling, and G. Pin, Appl. Phys. Lett. **98**, 109082 (2009).
4. M. Sumiya, Y. Kamo, N. Ohashi, et al., Appl. Surf. Sci. **256**, 4442 (2010).
5. A. Alexeev, D. Krasovitsky, S. Petrov, and V. Chaly, *Proceedings of the 16th European Molecular Beam Epitaxy Workshop (Alpe d'Huez, 2011)*, M3.3.
6. T. A. Komissarova, V. N. Jmerik, A. M. Mizerov, N. M. Shmidt, B. Ya. Ber, D. Yu. Kasantsev, and S. V. Ivanov, Phys. Status Solidi (c) **6** (S2), 466 (2009).
7. M. R. Ainbund, E. G. Vil'kin, A. V. Pashuk, A. S. Petrov, and I. N. Surikov, Tech. Phys. Lett. **30**, 451 (2004).
8. V. N. Jmerik, A. M. Mizerov, T. V. Shubina, A. V. Sakharov, A. A. Sitnikova, P. S. Kop'ev, S. V. Ivanov, E. V. Lutsenko, A. V. Danil'chik, N. V. Rzheutskii, and G. P. Yablonskii, Semiconductors **42** (12), 1420 (2008).
9. G. Pozina, P. P. Paskov, K. P. Bergman, C. Hemmingsson, L. Hultman, B. Monemar, H. Amano, and A. Usui, Appl. Phys. Lett. **91**, 221901 (2007).
10. J. K. Kim, E. L. Waldron, Y. -L. Li, Th. Gessmann, E. F. Schubert, H. W. Jang, and J.-L. Lee, Appl. Phys. Lett. **84**, 3310 (2004).
11. M. A. Reshchikov, G.-C. Yi, and B. W. Wessels, Phys. Rev. B **59** (20), 13 176 (1999).

Translated by P. Pozdeev